

Scale Invariance, Self Similarity and Critical Behavior in Classical and Quantum Systems

To cite this article: Irving O Morales *et al* 2012 *J. Phys.: Conf. Ser.* **380** 012020

View the [article online](#) for updates and enhancements.

Related content

- [Self similitude in the power spectra of nuclear energy levels](#)
V Velázquez, E Landa, C E Vargas et al.
- [Perspectives on \$1/f\$ noise in quantum chaos](#)
R A Molina, A Relaño, J Retamosa et al.
- [Fractal time series analysis](#)
A Eke, P Herman, L Kocsis et al.



IOP | ebooks™

Bringing you innovative digital publishing with leading voices to create your essential collection of books in STEM research.

Start exploring the collection - download the first chapter of every title for free.

Scale Invariance, Self Similarity and Critical Behavior in Classical and Quantum Systems

Irving O Morales

Instituto de Ciencias Nucleares, Universidad Nacional Autónoma de México, Apartado Postal 70-543, 04510 México, D.F., Mexico

E Landa

Instituto de Ciencias Nucleares, Universidad Nacional Autónoma de México, Apartado Postal 70-543, 04510 México, D.F., Mexico

R Fossion

Instituto de Ciencias Nucleares, Universidad Nacional Autónoma de México, Apartado Postal 70-543, 04510 México, D.F., Mexico

A Frank

Instituto de Ciencias Nucleares, Universidad Nacional Autónoma de México, Apartado Postal 70-543, 04510 México, D.F., Mexico

Abstract. Symmetry and self-affinity or scale invariance are related concepts. We explore the fractal properties of fluctuations in dynamical systems, using some of the available tools in the context of time series analysis. We carry out a power spectrum study in the Fourier domain, the method of detrended fluctuation analysis and the investigation of autocorrelation function behavior. Our study focuses on two particular examples, the logistic module-1 map, which displays properties of classical dynamical systems, and the excitation spectrum of a schematic shell-model Hamiltonian, which is a simple system exhibiting quantum chaos.

1. Introduction

The concept of symmetry is closely related to self-similarity. In a broad sense symmetry implies that a system under the action of some transformation remains invariant, i.e, the system remains similar (or identical) to itself. The concept of self-similarity in a more mathematical sense is related with a special case of transformation, the re-scaling of the system. A self-similar object is statistically (or exactly) similar to a part of itself, which in turn remains similar to a smaller part of itself, and so on. Fractals are systems which present such self-similar behavior and the examples in nature are many.

Coastlines and natural frontiers have been found to be *fractal*. A coastline is *scale invariant*, if it looks self-similar at any scale and does not have a characteristic length. Specifically, the

length of a coastline \mathcal{L} is a function of the length of the measuring rod l and follows a *power law* of the form [1, 2],

$$\mathcal{L} = l^{1-D}, \quad (1)$$

where D is the fractal dimension. A coastline with $D = 1$ would appear straight in the map, whereas a coastline with $D = 2$ would consist of an infinite self-similar sequence of bays within bays without upper or lower limits. Natural coastlines have a fractal dimension $1 < D < 2$.

We are interested in using the self-similarity of a dynamical system in order to study some of its properties. A *dynamical system* [3] can be any real or hypothetical system that evolves over time. Its mathematical description consists of a *state vector* (a set of real numbers) that describes the system's state in phase space, and a *function* or *rule* that governs in a deterministic way the evolution of the state vector in time. Many dynamical systems are composite systems, and consist of locally interacting parts. A *complex system* [4] is a special type of dynamical composite system, where under critical circumstances new collective behavior emerges from the short-range interactions between the constituent parts.

It is not always possible to fully determine all the components of the state vector of the dynamical system. However, an elegant way to study a large variety of dynamical systems is through the use of *time series*, that follow the evolution of a specific observable as a sequence of data points, typically measured at successive times spaced at uniform time intervals. Not only do time series offer valuable information on the internal dynamics of the systems that produce them, but have the additional advantage that the same theoretical methods can be used to analyze time series of very different systems. In this contribution we study time series associated with both classical and quantum systems, although in the latter case we shall actually use energy instead of time, as we explain below. Time series can be fractal, if segments of it remain self-similar at different time scales. An interesting example is provided by the heartbeat interval series, that remains self-similar for time scales ranging from 10 seconds up to several hours [5, 6].

If the time series is fractal, then the power spectrum $S(f)$ must also be scale invariant and behave as a power law,

$$S(f) \sim f^\beta, \quad (2)$$

where β is the *spectral density exponent*, with $\beta = 0$ for white noise and $\beta < 0$ for reddened noise. In a log-log representation, the power law translates into a straight line, with β as the slope. Such broadband power spectra, without a characteristic frequency, have indeed been observed for time series of a wide variety of dynamical systems, including the interval fluctuations of a healthy heart [7].

The spectral density exponent β is a measure of the amount of correlations present in the time series. There is no correlation for white noise ($\beta = 0$) and a large one for brownian noise ($\beta = -2$). The power-law behaviour of the power spectrum $P(f) \sim f^\beta$ of eq. (2) implies that the power spectrum of f^β noises is *scale invariant*. In white noise ($\beta = 0$), if one integrates the power of the power spectrum per frequency decade, then one finds that the contribution increases a factor ten per decade. White noise is convergent at small frequencies but diverges at higher frequencies. This translates into the fact that the mean value of a specific white-noise time-series converges as the value is averaged over longer and longer time intervals, but its instantaneous value is undefined. On the other hand, in brownian noise ($\beta = -2$), the power contribution decreases a factor of ten per decade. Brownian noise is convergent at higher frequencies but diverges at lower frequencies. A specific brownian time series is thus well defined at every single time, but it does not have a well defined mean value for large time intervals, as

the random-walk function wanders farther and farther away from the initial value. In the power spectrum of $1/f$ noise, every frequency decade contributes with exactly the same amount of power (proportional to $\log 10$) [8, 9], a perfect scaling property that we already recognized in the time scaling of the autocorrelation function, see eq. (6). $1/f$ noise thus constitutes a “golden mean”, in between white noise and brownian noise. The spectrum is divergent both towards low and high frequencies, and as a consequence a specific $1/f$ time series does not have a well-defined long-term mean nor a well-defined value at a single point. However, as the divergence is slow (logarithmic), frequency cutoffs can be applied to the power spectrum at low or high frequencies, without the time series changing its appearance [10].

In a sense, $1/f$ noise can be seen as the fingerprint of a system that has *maximized its efficiency* within its own limits. This statement is based on the assumption that a biological system operates so as to maximize its efficiency [9, 11], and on the empirical observation that many (if not all) biological time series that correspond to involuntary or autonomous signals display $1/f$ behavior when they are healthy. In contrast, with age, disease or bad habits a deviation from $1/f$ is observed towards either more random or more regular regimes. Health in biological systems is thought to function in a critical regime, characterized by $1/f$ signals.

It can be shown that the autocorrelation function $C(\tau)$ of these systems must also be scale invariant. This can be understood in the following way. According to the Wiener-Khinchin theorem, the autocorrelation function is the inverse Fourier transform of the power spectrum,

$$C(\tau) = F^{-1}(S(f)). \quad (3)$$

If the power spectrum obeys the power law of eq. (2), and we apply a scale transformation in the time domain, $\tau \rightarrow \tau' = a\tau$, then,

$$C(a\tau) = F^{-1}\left(\frac{1}{a} S\left(\frac{f}{a}\right)\right) = a^{-\beta-1} F^{-1}(f^\beta) = a^{-\beta-1} C(\tau), \quad (4)$$

and thus the autocorrelation function conserves its behavior after time transformations (up to a scaling factor $a^{-\beta-1}$). The general solution of this equation is that the autocorrelation function $C(\tau)$ itself is also a power law. White noise ($\beta = 0$) is a particular case, where

$$C(a\tau) = \frac{1}{a} C(\tau), \quad (5)$$

so that the autocorrelation function for white noise is a delta function, $C(\tau) = \delta(\tau)$, since delta functions obey the scaling law $\delta(a\tau) = |a|^{-1}\delta(\tau)$. Flicker noise or $1/f$ noise ($\beta = -1$) is another particular case, where

$$C(a\tau) = C(\tau), \quad (6)$$

with solutions $C(\tau) = \text{constant}$, or the physically more significant case $C(\tau) = -\log(\tau)$. Rescaling a logarithmic function gives $\log(a\tau) = \log(\tau) + \log(a)$, where $\log(a)$ is a constant that does not contribute to the time evolution of the autocorrelation function, so that the scaling relation of eq. (6) is approximatively satisfied, $C(a\tau) \cong C(\tau)$.

For discrete time series, apart from spectral analysis, there are other tools to study scale transformations, including the Detrended Fluctuations Analysis (DFA) method [12]. The DFA method is used to estimate long-range power-law correlation exponents in diverse kinds of signals [13]. In order to apply the DFA the time series is integrated and then divided into nonoverlapping N/l boxes of equal length containing l data points. Then a local trend is defined

for each box, i.e. a linear fit to the integrated time series. Then the variance between the integrated time series and the local fit is computed for each box and averaged over all the boxes of size l . The average variance $F(l)$ depends on the box size. The analysis of this dependence allows to study the scaling properties of the system and the presence of long-range correlations. A linear relationship between $\text{Log}(F(l))$ and $\text{Log}(l)$ will indicate a scaling behavior. The slope α_{DFA} in the $\text{Log}(F(l))$ vs $\text{Log}(l)$ plot characterizes the scaling properties of the time series because it reflects a power law of the form $F(l) \sim l^{\alpha_{\text{DFA}}}$. In the case of a regular uncorrelated system the theoretical value of the slope is $\alpha_{\text{DFA}} = 1/2$. The parameter α_{DFA} , obtained by means of the DFA, which in this case is related to the self-similarity properties, can be related with the exponent β of the spectral analysis through the simple relation

$$\beta = 2\alpha_{\text{DFA}} - 1, \quad (7)$$

valid in the range $0.5 < \alpha_{\text{DFA}} < 1.0$. The relationship between the exponent of the autocorrelation function γ and α_{DFA} is given by $\gamma = 2 - 2\alpha_{\text{DFA}}$ [14]. In particular, for time series with $1/f$ -noise ($\beta = 1$), $\alpha_{\text{DFA}} = 1$ and $\gamma \rightarrow 0$ (see e.g. [15]).

2. Module-1 Logistic Map

The *logistic map*, $x_{n+1} = kx_n(1 - x_n)$, is a map of the unit interval $[0,1]$ onto itself, which produces time series that are periodic or chaotic depending on the value of the control parameter $k \in \text{the interval } [0,4]$ [16]. Complex behavior, such as $1/f$, can only be expected at the *edge of chaos* at the borderline between two different regimes [17]. The *mod-1 map*, also called the *Manneville iteration map*, $x_{n+1} = x_n + kx_n^2(\text{Mod}1)$, on the other hand, produces self-affine time series and has been used as a model for intermittency (see Fig. 1). Moreover, the time series exhibit $1/f$ power spectral density for many values of its control parameter k [18, 19, 20, 21]. Both discrete maps belong to the class of discrete-time dynamical deterministic systems, corresponding to one-dimensional maps of a given interval, which are perhaps the simplest models displaying a sensitive dependence on initial data. We construct a new map, the *mod-1 logistic map*,

$$x_{n+1} = k(x_n + x_n^2)(\text{mod } 1), \quad (8)$$

where the dynamic behavior of the resulting time series depends on the value of the control parameter k . We focus on the behavior of the time series close to a particular point, where the system undergoes a sudden order to chaos transition for a minimal change of the control parameter. We study the dependence on initial conditions by repeated iteration of the map, Eq. (8), which yields a sequence where the value x_{n+1} at step $n + 1$ depends explicitly only on the value x_n of the previous step n , and maps the $[0, 1]$ interval onto itself. The changes in long-range correlations of the time series with this map are analyzed as the control parameter k is varied with steps of 0.0125. In the following, we consider ensembles for different values of k , with 10 different initial conditions and time series of length 3000. We present below the results for each ensemble. For $k < 1$, the time series x_n is a monotonic decreasing function that tends to zero after a few hundred iterations. For $k = 1$, the map corresponds to the original mod-1 map and the time series is thus self-affine and intermittent. For $k > 1$, the time series loses its intermittent behavior for increasing k . To quantify regular and chaotic behaviour, we calculate an estimated value for the Lyapunov exponent λ for the $x_n(k)$ time series as a function of k ,

$$\lambda(k) = \lim_{m \rightarrow \infty} \frac{1}{m} \sum_{n=0}^{m-1} \log |x'_{n+1}(k)|, \quad (9)$$

where $x'_{n+1} = k(1 + 2x_n)$ is the derivative of x_{n+1} of Eq. (8) with respect to the previous value x_n .

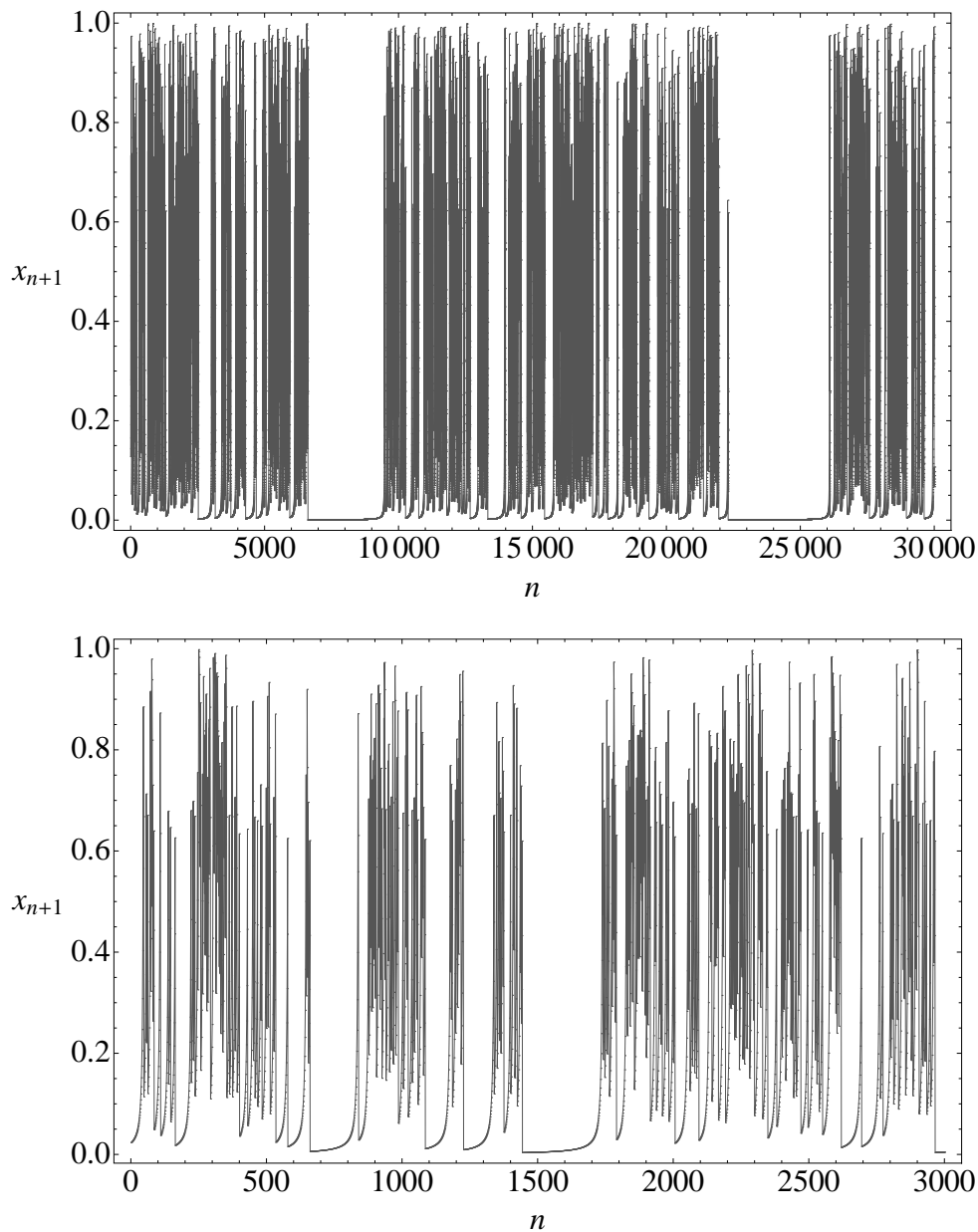


Figure 1: The self-affine time series of the Module-1 Logistic Map of eq. (8) with $k = 1$, consists of bunches of peaks (upper panel) that contain additional bunches on a smaller scale (bottom panel).

We obtain $\lambda < 0$ for $k < 1$, which confirms that the corresponding time series $x_n(k)$ are regular, whereas $\lambda(k) > 0$ for $k > 1$ indicates that the corresponding time series $x_n(k)$ are increasingly chaotic for larger k . The edge of chaos, $\lambda_k = 0$, is obtained for $k = 1$. We now study the evolution of the correlation strength of the time series $x_n(k)$ as a function of the control parameter, using spectral analysis and the DFA method, with the exponent β of Eq. (2) and $\beta = 2\alpha_{\text{DFA}} - 1$ of Eq. (7), respectively. For $k \neq 1$ ($k > 1$), the power spectral density flattens out at the smallest frequencies, and this flat part tends to be larger as k moves further away from 1, indicating that a portion of the large-range correlations are lost. We then study the part of the spectral density where the correlations are conserved. The spectral analysis and

the DFA give comparable results, see Fig. 2. We point out that before k acquires the value one, it does not make sense to fit the power spectral density for a periodic regime. On the other hand, for the chaotic time series $k > 1$, the non-flat part of the spectral density at higher frequencies loses gradually its correlation strength, $\beta \rightarrow 0$, (white-noise like) for larger k . At the edge of chaos, for $k = 1$, a $1/f$ behavior ($\beta = 1$) is observed that extends through the whole range of the frequencies. In conclusion, the transitional point $k = 1$ in this simple classical system in between regularity and chaos is characterized by long-range correlations of the $1/f$ type, whereas its limiting regimes are characterized by strong and weak correlation strengths, respectively, but with a shorter range.

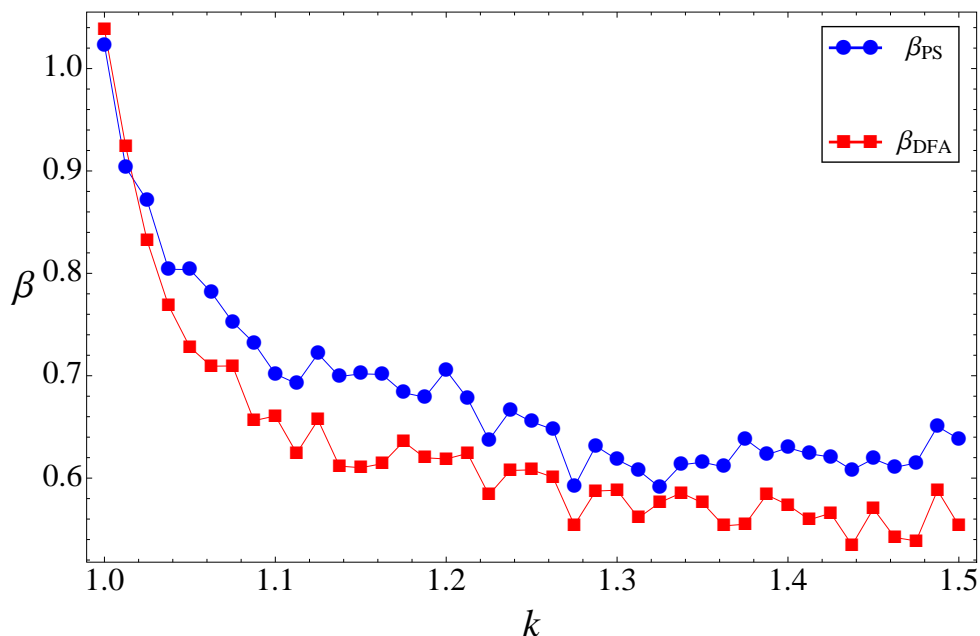


Figure 2: The correlation strength β of time series $x_n(k)$ as a function of k in the map of Eq. (8). The line connecting the blue dots is the spectral density exponent β (in the figure as β_{PS}) from Eq. (2), whereas the line connecting the red squares is $\beta = 2\alpha_{DFA} - 1$ (in the figure as β_{DFA}) from Eq. (7).

3. Quantum excitation spectra as a time series

3.1. Unfolding and fluctuations in the quantum spectra

Quantum chaos studies the correlations present in the excitation spectra of quantum systems, which correspond to a monotonic series of levels at increasing energies, E_1, E_2, E_3, \dots . In this case we analyse their *fluctuations* with respect to an equidistant (harmonic oscillator) energy spectrum. The procedure used to extract the information of the fluctuating part of the quantum spectrum is called *unfolding*: the global features of the energy level density are usually modeled by a smooth function, which is subtracted from the total level density to leave only the oscillating part. The unfolding is a delicate procedure [22, 23]. The level density is usually approximated by a smooth function (*e.g.* polynomial function) which can, however, affect the results, especially the sensitive long-range correlations [24]. Instead of following this procedure, in this paper we employ the Empirical Mode Decomposition (EMD) method to perform the unfolding procedure in quantum excitation spectra. This method originated in the theory of signal analysis, where

the determination of the trend and the corresponding detrending is a fundamental task. Following [25] we use a simple definition of the global trend for arbitrary nonlinear and non-stationary time series. One of the important properties of the method is its adaptability to a given time series. It can reveal natural time scales of the signal and is able to extract various trends at different time scales [25]. In this sense the EMD method interprets the trend as an integral part of the data, *i.e.* it is driven by the same mechanisms that give rise to the rest of the signal. Our unfolding procedure combines a small degree polynomial fit (fifth-order) to remove the basic trend of the data around their average, followed by the empirical mode decomposition, which subtracts the rest of the trend in a very accurate way. We have found that these procedure is independent of the degree of the original polynomial. A detailed analysis of the EMD method to determine the fluctuations in the quantum spectra has been recently published [26].

The fluctuations in the quantum spectra can be formally interpreted as a discrete time series [22] by using the quantity

$$\delta_n = \sum_{i=1}^n (s_i - \langle s \rangle) = [\epsilon_{n+1} - \epsilon_1] - n\langle s \rangle, \quad (10)$$

where $s_i = \epsilon_{i+1} - \epsilon_i$. The stochastic discrete function δ_n measures the deviations of the distance between the $(n + 1)$ -th unfolded state, with respect to the corresponding state in a uniform (equally spaced) sequence.

3.2. Energy fluctuations in shell model nuclear calculations

Following Relaño et al. [22], we use a spectral analysis to study the long-range correlations. We also apply the DFA method to the quantum spectral fluctuations, in a way similar to that of reference [27]. We performed calculations for large-scale shell-model calculations with realistic interactions (KB3) [28] in the full fp shell for ^{48}Ca in the subspaces $J^\pi = 0^+, 1^+, \dots, 8^+$ by means of the ANTOINE code [29]. In the present study we repeated the DFA and spectral analysis of the time series, but using the EMD procedure to improve the unfolding. We obtained a nearly $1/f$ power-law behavior, that is confirmed by results with $\alpha_{\text{DFA}} = 1$ for the DFA, the largest deviation being of $\sim 10\%$ (see Table 1). These results are in agreement with the ones of Relaño et al. and our previous results [24]. We also studied the energy fluctuations of the two-body random-ensemble (TBRE) [30, 31] shell-model calculations for ^{48}Ca in the subspace $J^\pi = 0^+$. We found $\beta = 1.01$ and $\alpha_{\text{DFA}} = 1.02$. This value is very similar to the case of realistic calculations that is shown in Table 1. Relaño *et al.* [22] performed the first study of the behavior of the power spectral density of the energy fluctuations of TBRE random shell-model calculations for ^{24}Mg and ^{32}Na and found that they obey a $1/f$ scaling.

3.3. Energy fluctuations in a phase-transitional model

Large-scale shell-model calculations and TBRE calculations carried out to describe real nuclei are found to produce $1/f$ time series, but these calculations are very complicated and involve many degrees of freedom. In this section, we use a schematic Hamiltonian in a simplified version of the shell model, with which we can follow a transition in-between different regimes, in order to study how the power spectral density evolves, with particular emphasis on what happens at the transitional point.

We use the Hamiltonian

$$H = H_0 + \chi \hat{Q} \cdot \hat{Q}, \quad (11)$$

Table 1: Self-similarity parameter α_{DFA} obtained using a linear DFA method, and the β exponent in the power spectral density of the energy fluctuations in the shell-model calculations of ^{48}Ca with realistic interactions in different subspaces J^π . The dimension N of each subspace is also shown. The unfolding was done using the EMD method.

^{48}Ca			
0^+	1.03	1.09	347
1^+	0.99	1.10	880
2^+	1.02	1.03	1390
3^+	1.04	1.13	1627
4^+	1.01	1.09	1755
5^+	1.10	1.13	1617
6^+	1.06	1.08	1426
7^+	1.03	1.05	1095
8^+	1.05	1.07	808

with an external adjustable parameter χ . This schematic Hamiltonian is analogous to simple boson Hamiltonians used recently to study quantum phase transitions [32]. The unperturbed single-particle (s.p.) Hamiltonian H_0 describes non-interacting fermions in the mean field of an appropriate spherical core which is known to be integrable [33]. The second term, $\chi \hat{Q} \cdot \hat{Q}$, describes a residual quadrupole-quadrupole two-body interaction, which in this case acts on 8 valence neutrons in the fp shell, and this part by itself is also integrable. We carry out calculations in the subspace $J^\pi = 3^+$ of ^{48}Ca . The coefficient χ in Eq. (11) modulates the intensity of the quadrupole-quadrupole interaction and gives rise to the level repulsion in the nuclear spectrum. Varying the intensity of this control parameter in the range $0.01 < \chi < 0.40$, we find that the power spectral density of the δ_n time series behaves as $P(f) \sim 1/f^\beta$ with $\beta=1.92$ (for $\chi = 0.01$), $\beta = 1.10$ (for $\chi = 0.21$) and $\beta = 1.43$ (for $\chi = 0.40$), values that are confirmed by an analysis with DFA, see Fig. 3.

The fluctuations in the quantum spectra with the realistic KB3 interaction are in good agreement with the spectral fluctuations obtained with the schematic Hamiltonian when the intensity parameter χ takes values close to 0.21. Thus, we find that the fluctuations of both integrable limits tend to approach a brownian-like $1/f^2$ power spectral density, whereas a density close to $1/f$ is found at the transitional point.

4. Conclusions

Self-similarity is a very important property of dynamical systems which can be analyzed using the usual tools of time-series analysis. For the dynamical systems presenting scale invariance the power spectral density behaves as a power law $P(f) \sim 1/f^\beta$. The $1/f$ noise ($\beta = 1$) can be seen as a particular type of self-similar noise. It corresponds to signals that maximize the range of their correlations. We suggest in this paper that time series of both classical and quantum dynamical systems that undergo a transition between two regimes, exhibit $1/f$ behavior near the transitional point. We report in detail on two specific examples: the Module-1 Logistic Map for the classical case, and a schematic nuclear shell-model Hamiltonian for the quantum case. We studied the corresponding time series by spectral analysis, and with the DFA method.

In the case of the module-1 logistic map, for values of the control parameter $k < 0$, we found regular time series (with Lyapunov exponent $\lambda_k < 0$), for a value of $k = 1$, a correlated

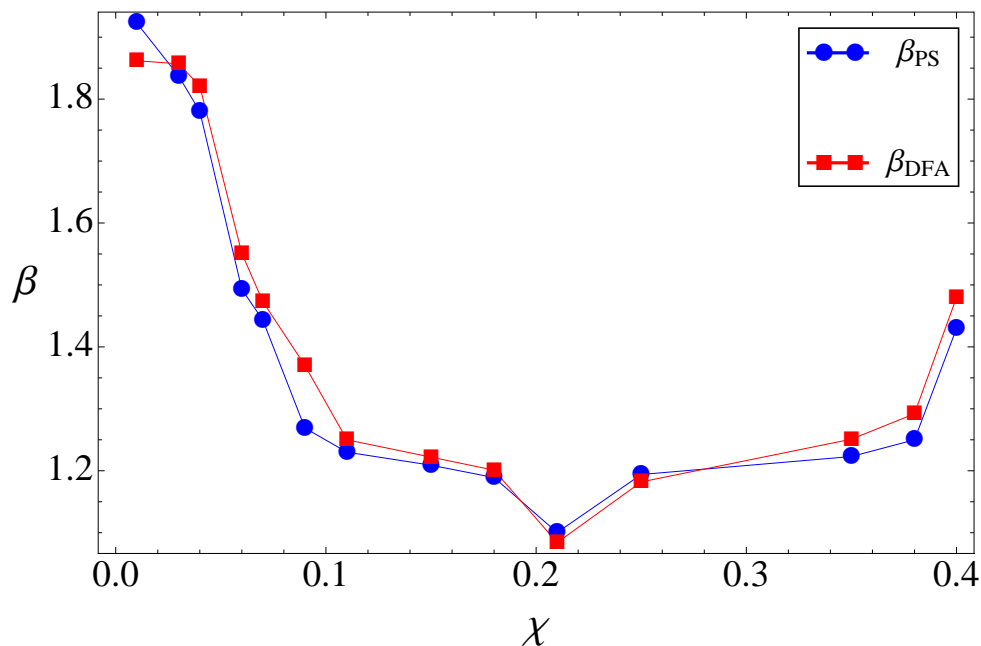


Figure 3: (Color online) The values of β calculated directly from the fit to the slope of the power spectral density (blue dots) to each δ_n in function of χ in the Hamiltonian of Eq. (11). The red squares are the β 's obtained using the relation with α_{DFA} .

non-periodic time series (with Lyapunov exponent $\lambda_k = 0$), and for control parameters $k > 1$ we observe chaotic time series (with Lyapunov exponent $\lambda_k > 0$). We find $1/f$ behavior for the correlated non-periodic time series at the transitional point, whereas the regular and chaotic time series correspond to $1/f^\beta$ ($\beta \neq 1$) power spectral density. We describe a generic nuclear excitation spectrum, using a schematic Hamiltonian. The Hamiltonian has two competing terms: a single-particle term, and a residual quadrupole-quadrupole term. Each term individually is integrable. A control parameter allows for a smooth transition between the two extreme regimes. Both extreme integrable excitation spectra correspond to $1/f^2$ (brownian) power laws, whereas the transitional excitation spectrum corresponds with a $1/f$ power spectral density. For two specific systems, we found a generic $1/f$ behavior of the corresponding time series, where the long-range correlations are maximized, exactly at the point where the transition occurs. We are currently applying these techniques to other systems, such as simple coupled pendula and photon counting rates in different kinds of emitting light sources [34]. We believe that time series analysis can provide relevant information in both physical and biological systems, including early warning signals in diverse phenomena [35].

Acknowledgements

We thank Pavel Stransky for his critical reading of this manuscript and his important comments. This work was supported in part by grants from CONACyT-Mexico, project I0017 - CB-2010-01 - 156663 and by the project FP7-PEOPLE-2009-IRSES-247541-MATSIQEL.

References

- [1] Richardson L F 1961 *General Systems Yearbook* **6** 139
- [2] Mandelbrot B 1967 *Science* **156** 636
- [3] Scheinerman E R 1995 *Invitation to Dynamical Systems* (Upper Saddle River, NJ: Prentice Hall) p 1
- [4] Bak P and Paczuski M 1993 *Physics World* (Dec 1993) 39
- [5] Goldberger A L, Rigney D R and West B J 1990 *Sci. Am.* **262** 34

- [6] Kaplan D T and Talajic M 1991 *Chaos* **1** 251
- [7] Goldberger A L Rigney D R, Mietus J, Antman E M and Greenwald M 1988 *Experientia* **44** 983
- [8] Halley J M 1996 *TREE* **11** 33
- [9] Halley J M and Inchausti P 1996 *Fluct. Noise Lett.* **4** R1
- [10] Press W H 1978 *Comments Astrophys.* **7** 103
- [11] Deering W and West B J 1992 *IEEE Eng. Med. Biol.* **11** 40
- [12] Peng C-K, Havlin S, Stanley H E and Goldberger A L 1995 *Chaos* **5** 82
- [13] Talkner P and Weber R O 2000 *Phys. Rev. E* **62** 150
- [14] Beran J 1994 *Statistic for Long-Memory processes* (New York: Chapman and Hall)
- [15] Montroll E W and Shlesinger M F 1984 in: *Nonequilibrium Phenomena II. From Stochastics to Hydrodynamics* (Amsterdam: North-Holland) p 1
- [16] May R M 1976 *Nature* **261** 459
- [17] Bak P 1996 *How Nature works* (New York: Springer-Verlag)
- [18] Milotti E 2002 *e-print physics/0204033*
- [19] Manneville P 1980 *J. Physique* **41** 1235
- [20] Ben-Mizrachi A, Procaccia I, Rosenberg N, Schmidt A and Schuster H G 1985 *Phys. Rev. A* **31** 1830
- [21] Procaccia I and Schuster H 1983 *Phys. Rev. A* **28** 1210
- [22] Relaño A, Gómez J M G, Molina R A, Retamosa J and Faleiro E 2002 *Phys. Rev. Lett.* **89** 244102
- [23] Brody T A, Flores J, French J B, Mello P A, Pandey A and Wong S S M 1981 *Rev. Mod. Phys.* **53** 385
- [24] Landa E, Morales I, Hernández C, López Vieyra J C, Frank A and Velázquez V 2008 *Rev. Mex. Fis.* **S-54** 48
- [25] Huang N E, Shen Z, Long S R, Wu M C, Shih E H, Zheng Q, Tung C C and Liu H H 1998 *Proc. R. Soc. Lond. A* **454** 903
- [26] Morales I O, Landa E, Stránský P and Frank A 2011 *Phys. Rev. E* **84** 016203
- [27] Santhanam M S, Bandyopadhyay J N and Angom D 2006 *Phys. Rev. E* **73** 015201(R)
- [28] Kuo T T S and Brown G E 1968 *Nucl. Phys. A* **114** 241
- [29] Caurier E, Zuker A P and Poves A 1991 in: *Nuclear Structure of Light Nuclei far from Stability. Experiment ad Theory, Proceedings of the Workshop, Obrnai, France, Nov. 27-29, 1989* ed G Klotz (Strasbourg: Kuster)
- [30] French J B and Wong S S M 1970 *Phys. Lett. B* **23** 449
- [31] Wong S S M and French J B 1972 *Nucl. Phys. A* **198** 188
- [32] Cejnar P, Jolie J and Casten R F 2010 *Rev. Mod. Phys.* **82** 2155
- [33] Caurier E, Martínez-Pinedo G, Nowacki F, Poves A and Zuker A P 2005 *Rev. Mod. Phys.* **77** 427
- [34] Landa E *Ph.D. Thesis* to be published
- [35] Scheffer M, Bascompte J, Brock W A, Brovkin V, Carpenter S R, Dakos V, Held H, van Nes E H, Rietkerk M and Sugihara G 2009 *Nature* **461** 7260